Original Paper

Lilia Benchikh*, Yazid Ait Ferhat, Melia Guessoum, Abdelhafid Merzouki and Yves Grohens

Cellulose nanocrystals (CNC) from Diss plant: bleaching treatment effect

https://doi.org/10.1515/ijmr-2024-0251
Received September 18, 2024; accepted January 8, 2025;
published online April 2, 2025

Abstract: In this work, we investigate the efficiency of different pretreatment methods and their impact on the characteristics of cellulose nanocrystals (CNC) extracted from the Diss plant, a widely available plant in the North African region. Two extraction methodologies were employed, focusing on the effects of bleaching treatments using hydrogen peroxide and sodium chlorite. Fourier transform infrared spectroscopy confirmed the effective removal of non-cellulosic materials, yielding CNCs with a cellulose I crystalline structure. The Zeta potential analysis revealed an increased presence of hydroxyl groups on the CNC surface. Scanning electron microscopy showed that CNCs tend to form agglomerates upon drying. Thermogravimetric analysis demonstrated that the CNCs exhibit considerable thermal stability, with degradation temperatures ranging from 100 °C to 350 °C.

Keywords: Cellulose nanocrystals; Whiskers; Bleaching treatment; Cellulose fiber; Biopolymer

1 Introduction

Cellulose, the most abundant natural polymer on Earth, is widely present in various biomasses[1,2] and highly sought after in several industrial applications from construction material, biomedical, paper, and textiles to modern cellophane films, dietary fibers, and advanced chemicals. Recent decades have seen a shift in cellulosic research towards the nano scale, exploring the potential of cellulose microfibrils at the nanometer level.[3]

The study of cellulose since its discovery in 1864 has shown that cellulose microfibrils have disordered regions and highly ordered regions. In the crystalline regions, cellulose chains are closely packed together by strong and highly intricate intra- and intermolecular hydrogen-bonds, while the amorphous domains are regularly distributed along the microfibrils.[2] This semi-crystalline structure confers on cellulose the ability to provide nanocellulose on different types including cellulose nanofibers CNF, cellulose nanocrystals CNC, and bacterial nanocellulose BNC.[4,5]

CNCs sparked significant scientific interest for their exceptional characteristics such as a high modulus of elasticity as well as a specific surface of several hundred $m^2\,g^{-1}$. In addition, hydroxyl groups on the CNC's surface offer the opportunity to obtain chemically modified nanocellulose. These characteristics have encouraged their use in new applications such as electronics, construction, packaging, food, energy, health care, automotive, and aerospace.[3,6,7]

Researchers explored various lignocellulosic sources such as wood, pulps, bagasse, cotton, and recycled paper for CNC production. Additionally, new raw materials, extraction methods, surface modifications, and the environmental impact of CNCs have become areas of active research.[1,8] The type of raw material used for CNC production not only influences CNC's dimensions but also dictates the selection of appropriate pretreatment methods. Studies have shown that both the yield and properties of CNCs are heavily dependent on the source of cellulose and the specific treatment conditions employed, including treatment time and temperature, as well as the initial acid concentration.[9] Thus, regardless of the raw materials used, there are CNCs extraction several general steps to follow, involving cutting the raw materials into small pieces, removing the non-cellulose components (such as hemicellulose and lignin) by bleaching, alkali treatment and washing processes. The same pretreatment can be repeated multiple times to completely remove the

***Corresponding author: Lilia Benchikh**, Centre de Recherche en Technologies Agro-Alimentaires. Route de Targa Ouzemmour, Campus Universitaire, Bejaia, 06000, Algeria, E-mail: lilia.benchikh@crtaa.dz. https://orcid.org/0000-0003-4205-8289
Yazid Ait Ferhat, Mechanics Research Center, 25000, Constantine, Algeria, E-mail: aitferhatyazid@gmail.com
Melia Guessoum and Abdelhafid Merzouki, Laboratoire Physico-Chimie des Hauts Polymères, Université Ferhat Abbas, Setif 1, Setif, 19000, Algeria, E-mail: guessoum_melia@yahoo.fr (M. Guessoum), hafid_merzouki@yahoo.fr (A. Merzouki)
Yves Grohens, Institut de Recherche Dupuy de Lôme, Université de Bretagne Sud, UMR CNRS 6027, Lorient, France, E-mail: yves.grohens@univ-ubs.fr

non-cellulose compositions. Extra steps are usually needed to clean up the chemical residues after pretreatments.[1,10,11]

Several chemical, mechanical, biological, or combined processes are available for extracting cellulose from biomass, facilitating its transformation into nanofibers.[12,13] Alkaline treatments dissolve structural linkages between lignin and carbohydrates through the saponification of intermolecular ester bonds, leading to the disruption of the lignin and deacetylation of hemicellulose. This reduces molecular weight and increases solubility. Moreover, alkaline conditions cause the cellulose matrix to swell and the ionization of hydroxyl groups introduces negative charges.[14] After alkaline treatment, bleaching processes lead to the delignification of alkaline fibers by breaking down phenolic compounds with chromophoric groups.[14] The compounds used for fiber pretreatment include alkaline agents (NaOH, KOH, NH_4OH, and hydrazine), oxidizing agents (H_2O_2, $C_2H_4O_3$, ozone, oxygen, TEMPO, NaClO, and $NaClO_2$), organic solvents (acetone, methanol, ethanol, and ethylene glycol), and ionic liquids.[15] The most common bleaching process involves $NaClO_2$, where chlorine dioxide (ClO_2) released from $NaClO_2$ reacts with lignin to form lignin chloride in the presence of an acidic buffer. This lignin chloride loses its ability to bind with α-cellulose molecules and precipitates.[16] However, this method has a significant impact on human health and the environment.[17] Consequently, numerous chlorine-free treatments have been developed to mitigate its environmental effects.[12] Studies in the literature have replaced conventional chlorine-based methods with alternatives involving hydrogen peroxide and various organic and inorganic acids.[17] Hydrogen peroxide is an environmentally friendly and effective bleaching agent for removing lignin from ligno-cellulosic fibers.[16]

A study investigated various pretreatment techniques and their effects on the properties of cellulose nano-fibers (CNFs). They found that alkaline treatment with tetraacetylethylenediamine (TAED) followed by hydrogen peroxide bleaching achieved a crystallinity index exceeding 80 % and produced CNFs with a diameter of 20 nm.[13] Additionally, an alkaline pretreatment prior to hydrolysis has proven to be effective and essential in eliminating secondary reactions that may cause unwanted discoloration of nanocrystals.[17] Alkali and bleaching processes are adapted based on the specific proportions of cellulose, hemicellulose and lignin present in each type of fiber.[16]

After elimination of non-cellulosic materials, nanocellulose extraction will be done. In this context, acid hydrolysis, alkaline and oxidative degradation processes were found to be the most effective routes to extract highly crystalline cellulosic microfibrils.[1,10,11]

Acid hydrolysis is the leading method for extracting cellulose nanocrystals (CNCs). This process uses a strong acid to break down the amorphous (non-crystalline) regions of cellulose, exposing the highly crystalline cellulose fibrils. These individual crystallites form stable suspensions. Many studies have aimed at optimizing the production conditions to enhance the performance of the resulting CNCs.[1,10,11]

Therefore, one of the most important sources of cellulose remains wood, however the use of annual plants can be used as an alternative to wood for cellulose-based materials. These plants are interesting because of their abundance, low cost and their rapid growth which makes them available in many regions of the world.[18]

The *Ampelodesmos mauritanicus* or *Mauritanian* grass plant, commonly known as Diss in Arabic, is a grass plant of the family *Gramineae* largely present in the Mediterranean area and, in particular, North Africa and is abundantly available throughout the year. It grows in wet and dry areas which make them available for cultivation in rainfed systems and marginal lands. The average height of the *A. mauritanicus* plant can exceed one m, and their fibres are extremely sturdy and rough. The main constituents of *A. mauritanicus* are 44–46 % α-cellulose, 26–27 % hemicelluloses, 17–25 % lignin and 1.3 % fats and waxes, with a variable mineral content (SiO_2, Al_2O_3, Fe_2O_3, CaO, Na_2O and K_2O) (8–10 %), depending on the plant development conditions, composition of the soil, and growth climatic conditions.[19]

Its antiparasitic property represents a traditional use of this plant, while additional possibilities are in the manufacture of artisanal baskets and as traditional building material for roofs of old houses thanks to their mechanical and hydrous qualities. Very limited information is available in the literature on the mechanical and thermal properties of Diss fibers and the exploitation of these wild plant fibers as a reinforcement to cementitious composites and polymer composites is rarely studied.[20] *A. mauritanicus* fibers were incorporated in polyester matrix up to 30 % and a clear improvement in the mechanical proprieties of composite was achieved.[21] Recently, Bourahli[22] have carried out an in-depth study of Diss fibers in which their chemical compositions and the tensile strength were determined. Furthermore, Bourahli[22] found that the incorporation of Diss fibers into a polyester matrix led to an improvement of the matrix mechanical properties. Lately, another study, investigated the effect of various treatments and the fibers loading rate on the physical, mechanical and ther-mal properties of the composite Diss fibers/cement.[23] Also, Sarasini et al.[24] studied the reinforcement of PP and PLA matrix by Diss fibers.

In another study, the authors extracted the flavonoids from the aerial parts of *A. mauritanicus* and examined antibacterial activity *in vitro* using the disc diffusion method, they observed an inhibition of the growth of *Escherichia coli*

and *Staphylococcus saprophyticus* but was moderately active against *Pseudomonas aeruginosa* and *Staphylococcus epidermidis*.[21]

This study investigates two different extraction methods for cellulose nanocrystals (CNCs) from a local raw fiber *A. mauritanicus* (Diss) using hydrogen peroxide (H_2O_2) and sodium chlorite ($NaClO_2$). The methods will be referred to as CNC_{DH} and CNC_{DN}, respectively. The research focuses on how the chosen parameters within each extraction method affect the final CNCs. The dimensional, microstructural, and thermal properties of the both CNC_{DH} and CNC_{DN} will be compared and reported.

2 Experiments and materials

2.1 Materials

CNCs were extracted from Diss plant collected from Setif (Algeria). The used reagents were acetone (CH_3COCH_3), sodium hydroxide (NaOH), acetic acid (CH_3CO_2H), sodium chlorite ($NaClO_2$), and sulfuric acid (H_2SO_4) purchased from Sigma-Aldrich (St. Louis, Missouri, United States). Ethanol (CH_3CH_2OH) and Hydrogen peroxide (H_2O_2). All were purchased from Biochem Chemopharma (Montreal, Quebec, Canada).

2.2 CNC's extraction

The Diss plant was washed, dried and powdered, then treated with two extraction protocol as follow. This process is outlined in Figure 1. The mass ratio of fiber to solution was 1:20.

A wash with distilled water was carried out after each treatment and the temperature of the reactions was maintained in a water bath, conducted under magnetic stirring.

2.2.1 Method I

- **Alkaline treatment**: The Diss powder was treated with a solution of NaOH (5 %) at 70 °C for 1 h; this step was repeated 3 times.
- **Bleaching**: The treated Diss powder was then bleached with a solution of H_2O_2 (20 %) at 45 °C for 45 min.
- **Acid hydrolysis**: The bleached Diss powder was then hydrolyzed with a solution of H_2SO_4 (40 %) at 45 °C for 45 min, then a solution of NaOH (1 %) was added to the obtained solution with the hydrolysed powder.
- **Centrifugation**: To remove the container acid, the hydrolyzed Diss powder was then centrifuged at 4,000 rpm for 10 min.

2.2.2 Method II

- **Alkaline treatment**: The Diss powder was subjected to a mixture of CH_3COCH_3 and CH_3CH_2OH (38/62; V/V) for 24 h at room temperature, then with a solution of NaOH (3 %) at 80 °C for 2 h, carried out 5 times.
- **Bleaching**: The treated Diss powder was then bleached with a solution (50/50;V/V) consisting of 17 g of sodium chlorite $NaClO_2$ diluted in 1 L H_2O + 27 g NaOH diluted in

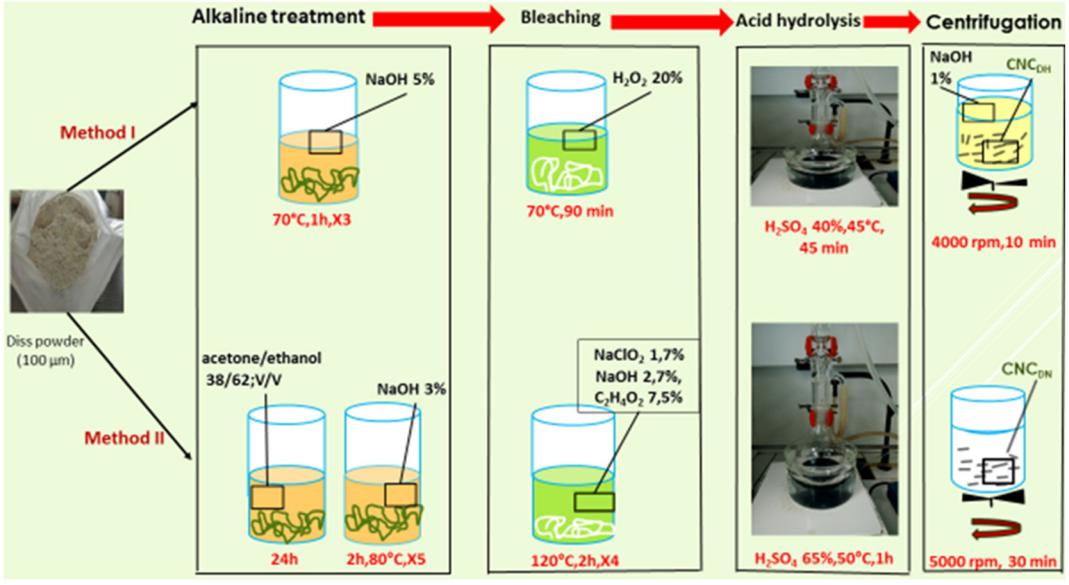

Figure 1: CNC_{DH} and CNC_{DN} extraction methods.

1 L H_2O and 75 ml of glacial acetic acid, at 120 °C for 2 h, then repeated 4 times.

- **Acid hydrolysis**: The bleached Diss powder was then hydrolyzed with a solution of H_2SO_4 (65 %) at 50 °C for 1 h.
- **Centrifugation**: The hydrolyzed Diss powder was then centrifuged at 5,000 rpm for 30 min.

2.3 Ultrasound treatments

To achieve a stable solution and improved dispersion of CNCs, CNC_{DH} and CNC_{DN} solutions (0.4 % mass concentration) were subjected to ultrasound treatment using a 20 kHz frequency ultrasonic generator for 120 min in a water bath with a Vibra-Cell™ VC 75185 Ultrasonic Processor (130 W) Thermo Fisher Scientific Inc., Waltham, MA, US.

2.4 Characterization techniques

2.4.1 Fourier transform infrared spectroscopy

The effectiveness of CNC extraction and the removal of non-cellulosic components from Diss fibers were assessed using Fourier transform infrared spectroscopy (FTIR). The samples were analyzed using a Vertex 70v FTIR apparatus (Bruker Corporation, Billerica, MA, USA). FTIR spectra are recorded in absorbance mode, between 4,000 cm^{-1} and 400 cm^{-1} with a resolution of 4 cm^{-1}.

2.4.2 Zeta-sizer analysis

CNC's surface charges were evaluated using zeta potential. The analysis was realized using DLS (Zeta-sizer nano ZS instrument).

2.4.3 Scanning electronic microscopy

Morphological characterization of CNC_{DH} and CNC_{DN} was performed with a scanning electronic microscope (SEM) using a JSM-6460 apparatus (JEOL Inc., MA, USA).

2.4.4 Thermogravimetric analysis

CNC's thermal behavior was studied using a Mettler Toledo thermogravimetric analysis (TGA)/differential scanning calorimetry (DSC) apparatus (Columbus, Ohio, USA) with a temperature interval [20–700 °C], a heating rate of 10 K min^{-1} and nitrogen environment (purge rate details: balance chamber flow rate ¼ 30 cm^3 min^{-1} and furnace flow rate ¼ 150 cm^3 min^{-1}).

3 Results and discussion

3.1 Structural analysis

The formation mechanism of CNCs through acid-catalyzed hydrolysis involves hydrogen ions from acids primarily attacking the glycosidic bonds between monosaccharide units. The crystalline regions remain intact, whereas the amorphous regions are broken down during hydrolysis.[25]

The hydrolysis reaction of cellulose fibers by sulfuric acid is depicted in Figure 2. Additionally, the chemical modifications of cellulose fibers after exposure to sulfuric acid and hydrolysis conditions are confirmed by FTIR analysis, as shown in Figure 3.

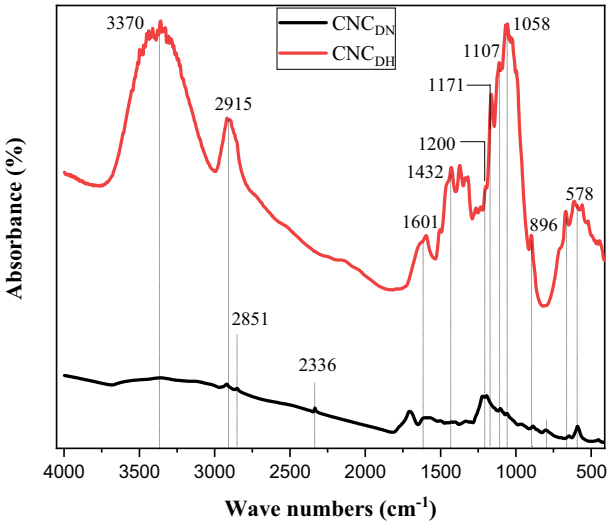

Figure 3: CNC_{DN} and CNC_{DH} FTIR spectra.

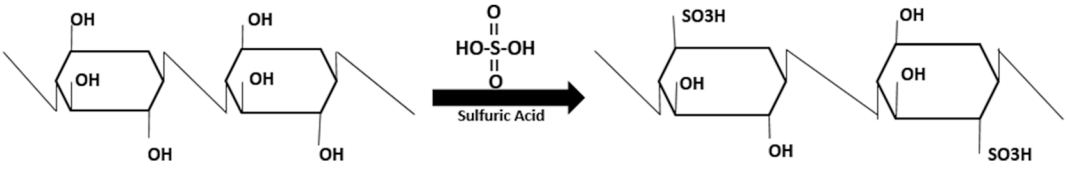

Figure 2: Cellulose acid hydrolysis reaction via sulfuric acid.

The FTIR spectra reported of CNC_{DN} and CNC_{DH} are symmetric and similar to those of previous studies.[26] The absorption bands characteristic of CNCs at 1,110 and 1,060 cm^{-1}, corresponding to skeletal vibrations of C–O stretching and the peak at 1,161 cm^{-1}, according to asymmetric stretching of C–O–C of glucose ring, confirm their cellulosic structure.[25,27–29] Additionally, the presence of signals at 1,432, 1,171, 1,107, and 896 cm^{-1} indicates that the CNCs mainly exhibit a cellulose I microstructure.[30] The absorption band at 711 cm^{-1} is assigned to Iβ cellulose, while the band at 750 cm^{-1}, attributed to Iα is non-existent.[31] Under the conditions of acid hydrolysis, cellulose microfibrils remain unaffected, and the nanoscale nature of cellulose nanocrystals is confirmed by a band around 800 and 896 cm^{-1}, attributed to C–O–C asymmetric elongation of the glucose ring in the cellulose structure. This band appears for both types of CNCs but is very weak for CNC_{DH}. Modification of cellulose with sulfuric acid is confirmed by the appearance of two new bands at around 1,200 cm^{-1}, attributed to sulphate half-ester groups.[32] The CNC_{DN} FTIR spectra show a wider band between 3,000 and 3,700 cm^{-1}, corresponding to OH group elongation vibrations, compared to that observed for CNC_{DH}. This indicates a higher cellulose content and a large amount OH groups formation due to the breakdown of β-1,4-glucosidic bonds.[33] According to previous studies,[34,35] the shapes of absorption bands before and after hydrolysis appearing around 4,000–2,995, 2,900, 1,430, 1,375 and 900 cm^{-1} are often used to indicate molecular order, where a wider band indicates a more disordered morphology. It can be observed that the OH groups band is clearer for CNC_{DH} compared to CNC_{DN}, suggesting that the hydrolysis parameters for CNC_{DN} affect the crystalline regions in addition to eliminating amorphous parts, leading to a more disordered material. The evaluation of absorbance band ratios at the wavenumbers 1,432 and 888 cm^{-1} is a method for comparing the crystallinity indices of CNC_{DN} and CNC_{DH}.[36] The results estimate a value of 1.125287 for CNC_{DN} and 1.349583 for CNC_{DH}, confirming previous results for CNC_{DH}. This allows us to deduce that the alkaline treatments undergone by CNC_{DN} allow a better diffusion of sulfuric acid during hydrolysis, leading to the complete elimination of the amorphous parts in cellulosic fibers. Previous studies have indicated a functionalization maximum of 1.5 on the C6, C2, and C3 carbons on the surface of a cellobiose unit.[37]

3.2 Zeta potential

Hydrolysis by sulfuric acid may eliminate the amorphous parts, retaining only the crystalline parts of the fibers. This process induces sulfate groups on the surface and substitutes hydroxyl groups with sulfate esters (SO^{-3}) creating electric charges that lead to an electrostatic repulsion. This repulsion helps prevent particle aggregation and contributes to a stable CNC solution.[38] The surface charges on CNCs are quantified by zeta potential measurements. Zeta potential results indicate that CNC_{DN} and CNC_{DH} exhibit negative surface charges of approximately −39.8 mV and −11.9 mV, respectively. The higher zeta potential of CNC_{DN} compared to CNC_{DH} suggests that CNC_{DN} is less prone to aggregation.[39] This is attributed to the higher number of hydroxyl groups on the CNC_{DN} surface, as indicated by previous FTIR results. These hydroxyl groups are more susceptible to esterification by sulfate ions. The low zeta potential value of CNC_{DH} is explained by the neutralization of negative charges after adding 1 % NaOH to the solution. Neto et al.[31] note that the zeta potential may depend on particle shape, size, and structure, which are influenced by hydrolysis conditions.[40] In this context, Nath and Pachuau,[41] obtain a zeta potential of about −6.3 mV for CNCs attributing it to particle aggregation after storage. It is also reported that severe acid hydrolysis conditions can result in a higher esterification rate.[28,42] This suggests that the hydrolysis conditions for CNC_{DH} are not sufficient to achieve a high esterification rate of hydroxyl groups by sulfate ions.

3.3 Morphological analysis

For further estimation of aggregation morphology and particle sizes of CNC_{DN} and CNC_{DH}. SEM analysis was conducted, and the results are reported in Figure 4.

SEM images for CNC_{DN} and CNC_{DH} indicate that CNC_{DN} surfaces are smoother and have fewer cavities, suggesting effective hydrolysis in removing extra cellulose substances and achieving nanoscale CNCs. Pandi et al.[43] report obtaining spherical nanoparticles between 20 and 100 nm with 50 % acid concentration, whereas an acid concentration of 30 % was insufficient to remove the complete amorphous phase from cotton, leading to higher cluster formation and CNC sizes ranging from 500 to 800 nm. The controlled diffusion nature of hydrolysis is specific to each fiber type and extraction protocol. These same results have already been reported by many authors.[32,44] Additionally, it is noted that after drying CNCs, hydrogen bond interactions between the particles increase. During drying, the forces from water elimination and high temperatures lead to molecular contact between CNCs, causing agglomeration due to hydrogen bond formation.[45] These interactions depend on the CNC source and the extraction methodology.[10,26]

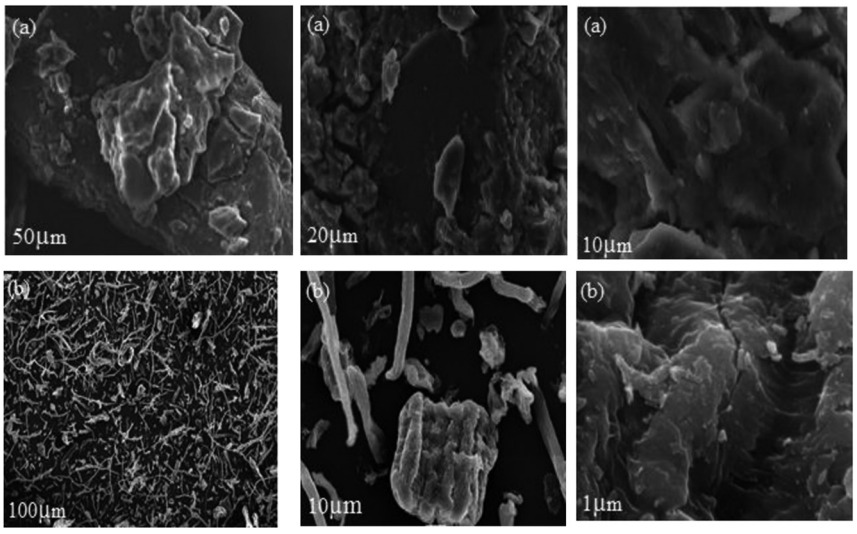

Figure 4: SEM micrographs: (a) CNC_{DN} and (b) CNC_{DH}.

3.4 Thermal stability

A thermogravimetric analysis was conducted to compare the thermal degradation of CNC_{DN} and CNC_{DH} obtained by different pretreatments. The analysis was based on weight loss (TG) thermograms and the derivatives of weight loss as a function of time (DTG), as shown in Figure 5.

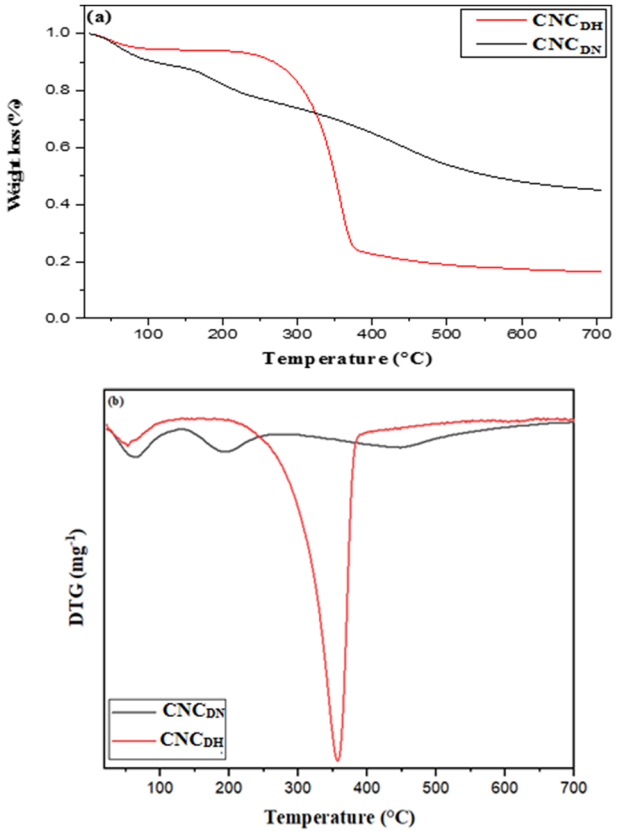

Figure 5: CNC_{DH} and CNC_{DN}: (a) TG, (b) DTG curves.

The CNC thermograms show three main decomposition stages. The first weight loss for both CNC_{DN} and CNC_{DH} occurs between 50 °C and 100 °C, attributed to evaporation of absorbed water.[46,47] The water fraction is larger for CNC_{DN}, indicating a higher concentration of –OH groups, consistent with FTIR and Zeta potential results.[26] CNC_{DN}'s primary pyrolysis begins around 195 °C, primarily due to the decomposition of sulfated amorphous regions. This temperature is significantly lower than the decomposition temperature of Diss cellulose (320 °C).[27] The substitution of hydroxyl groups by sulfate groups significantly decreases the activation energy for the degradation process, reducing the thermal stability of cellulose.[48,49] CNCs with a larger surface area are more exposed to heat and a free volume increase around the highly sulfated regions zones, resulting in a higher thermal conductivity.[8,32] In contrast, CNC_{DH} does not display primary pyrolysis, which can be explained by the lack of esterification on its surface, as indicated by zeta potential results. The second pyrolysis stage for CNC_{DN} and CNC_{DH} begins around 450 °C and 350 °C, respectively, corresponding to the decomposition of non-sulfated crystals.[50] CNC_{DN} and CNC_{DH} exhibit thermal stability between 100 and 220 °C and 100–350 °C, respectively. These findings for CNC_{DN} align with the results reported by Varma et al.[51] The thermal decomposition of CNC_{DH} is close to that of Diss cellulose, indicating that paracellulosic materials are not completely eliminated. This suggests that the pretreatment and hydrolysis conditions for CNC_{DN} result in nanocrystals with nanometric distribution and a surface rich in hydroxyl groups compared to CNC_{DH}.

Table 1 reports a comparison of the thermal properties and zeta potential of the CNCs obtained in this study with those reported in previous studies.

Table 1: Zeta potential and thermal stability for CNC_{DN} and CNC_{DH} comparison with previous studies.

Source	Zeta potential (mV)	ATG (°C)	Reference
CNCDN	−39.8	220	–
CNCDH	−11.9	350	–
Empty fruit bunch	−10	403.09	52
Filter paper	−40.5	290	53
Wood pulp	−39.8	301	53
Cotton	–	240	54

4 Conclusions

In the present study, CNCs were extracted from abundant local plants "Diss" by two extraction protocols to obtain CNC_{DH} and CNC_{DN}, respectively. Our findings confirm that the hydrolysis process selectively breaks down amorphous regions of cellulose fibers, preserving the crystalline regions and introducing sulfate ester groups on the CNC surface. This modification results in negatively charged CNCs, with zeta potential measurements indicating that CNC_{DN} has a higher charge than CNC_{DH}, making it less prone to aggregation and enhancing its dispersion stability. The results of the FTIR analysis show the total elimination of paracellulosic substances and the partial esterification of CNC_{DH} relatively to CNC_{DN}, demonstrating a higher nanometric scale distribution and surface esterification. The crystallinity index, as determined by absorbance band ratios, indicates that CNC_{DH} retains more crystalline regions compared to CNC_{DN}, exhibiting a more disordered morphology due to the removal of amorphous components. SEM images of CNC_{DN} and CNC_{DH} particles show high aggregation rate and sizes. The presence of the sulfate groups on the surface of the CNCs generated a lower thermal stability compared to the corresponding native fibers as was deduced from the TGA analysis.

These results highlight the significant impact of strong alkali treatment with $NaClO_2$ compared to H_2O_2 on the structural and chemical properties of CNCs. Thus, the processing parameters for extra cellulosic materials elimination and method of obtaining of the CNCs significantly influence the final properties of CNCs.

Research ethics: Not applicable.
Informed consent: Not applicable.
Author contributions: All authors have accepted responsibility for the entire content of this manuscript and approved its submission.
Use of Large Language Models, AI and Machine Learning Tools: None declared.
Conflict of interest: The authors state no conflict of interest.
Research funding: None declared.
Data availability: Not applicable.

References

1. Huang, S.; Liu, X.; Chang, C.; Wang, Y. Recent Developments and Prospective Food Related Applications of Cellulose Nanocrystals: A Review. *Cellulose* **2020**, *27* (6), 2991–3011. https://doi.org/10.1007/s10570-020-02984-3.
2. Park, N. M.; Choi, S.; Oh, J. E.; Hwang, D. Y. Facile Extraction of Cellulose Nanocrystals. *Carbohydr. Polym.* **2019**, *223*, 115114. https://doi.org/10.1016/j.carbpol.2019.115114.
3. Shojaeiarani, J.; Bajwa, D. S.; Chanda, S. Cellulose Nanocrystal Based Composites : A Review. *Compos. C: Open Access* **2021**, *5*, 100164. https://doi.org/10.1016/j.jcomc.2021.100164.
4. Philipp, H. J.; Nelson, M. L.; Ziifle, H. M. Crystallinity of Cellulose Fibers as Determined by Acid Hydrolysis. *Text. Res. J.* **1947**, *17* (11), 585–596. https://doi.org/10.1177/004051754701701101.
5. Mu, R.; Hong, X.; Ni, Y.; Li, Y.; Pang, J.; Wang, Q.; Xiao, J.; Zheng, Y. Recent Trends and Applications of Cellulose Nanocrystals in Food Industry. *Trends Food Sci. Technol*. **2019**, *93*, 136–144. https://doi.org/10.1016/j.tifs.2019.09.013.
6. Dufresne, A. Cellulose Nanomaterial Reinforced Polymer Nanocomposites. *Curr. Opin. Colloid Interface Sci*. **2017**, *29*, 1–8. https://doi.org/10.1016/j.cocis.2017.01.004.
7. Anžlovar, A.; Kunaver, M.; Krajnc, A.; Žagar, E. Nanocomposites of LLDPE and Surface-Modified Cellulose Nanocrystals Prepared by Melt Processing. *Molecules* **2018**, *23* (7), 1782. https://doi.org/10.3390/molecules23071782.
8. Mao, J.; Abushammala, H.; Brown, N. Comparative Assessment of Methods for Producing Cellulose I Nanocrystals from Cellulosicsources. In *Nanocelluloses: Their Preparation, Properties, and Applications;* Atalla, R. H.; Isogai, A., Eds.; ACS Symposium Series: Washington, DC, 2017, pp. 19–53.
9. Douard, L.; Bras, J.; Encinas, T.; Belgacem, M. N. Natural Acidic Deep Eutectic Solvent to Obtain Cellulose Nanocrystals Using the Design of Experience Approach. *Carbohydr. Polym.* **2021**, *252*, 117136. https://doi.org/10.1016/j.carbpol.2020.117136.
10. Habibi, Y.; Lucia, L. A.; Rojas, O. J. Chemistry, Self-Assembly, and Applications. *Chem. Rev.* **2009**, *110* (6), 3479–3500. https://doi.org/10.1021/cr900339w.
11. Dufresne, A. Polysaccharide Nanocrystal Reinforced Nanocomposites. *Can. J. Chem*. **2008**, *86* (6), 484–494. https://doi.org/10.1139/v07-152.
12. Trache, D. J.; Hussin, M. H.; Haafiz, M. K. M.; Thakur, V. K. Recent Progress in Cellulose Nanocrystals: Sources and Production. *Nanoscale* **2017**, *9* (5), 1763–1786; https://doi.org/10.1039/c6nr09494e.
13. Fernandes, A.; Cruz-Lopes, L.; Esteves, B.; EvtuguinD Nanotechnology Applied to Cellulosic Materials. *Materials* **2023**, *16* (8), 3104. https://doi.org/10.3390/ma16083104.
14. Hu, M.; Lv, X.; Wang, Y.; Zhang, Y.; Dai, H. Guideline for the Extraction of Nanocellulose from Lignocellulosic Feedstocks. *Food Biomacromol.* **2024**, *1* (1), 9–17; https://doi.org/10.1002/fob2.12011.
15. Zuliat, F. A.; Suardi, M.; Djamaan, A. CNC (Cellulose Nanocrystals) Isolation from Various Agriculture and Industrial Waste Using Acid Hydrolysis Methods. *IOSR J. Pharm. Biol. Sci.* **2021**, *15* (6), 42–58; https://doi.org/10.9790/3008-1506034258.
16. Nagarajan, K. J.; Ramanujam, N. R.; Sanjay, M. R.; Siengchin, S.; Surya, R. B.; Basha, K. S.; Madhus, P.; Raghav, G. R. A Comprehensive

Review on Cellulose Nanocrystals and Cellulose Nanofibers: Pretreatment, Preparation, and Characterization. *Polym. Compos* **2021**, *42* (4), 1588–1630; https://doi.org/10.1002/pc.25929.
17. Hafemann, E.; Battisti, R.; Bresolin, D.; Marangoni, C.; Machado, R. A. F. Enhancing Chlorine-free Purification Routes of Rice Husk Biomass Waste to Obtain Cellulose Nanocrystals. *Waste Biomass Valori* **2020**, *11* (12), 6595–6611. https://doi.org/10.1007/s12649-020-00937-2.
18. Chenah, M.; Amrani, M. Structural, Anatomy Characteristics and Thermal Properties of Ampelodesmos Mauritanicus (Diss). *Acta Sci. Agric.* **2020**, *4* (2), 92–97; https://doi.org/10.31080/ASAG.2020.04.0779.
19. Benhathat, A.; Amrani, M. Phosphate Removal from Water Using Activated Carbon Derived from *Ampelodesmos Mauritanicus* Stems: Equilibrium and Kinetic Studies. *Desalin. Water Treat.* **2021**, *234*, 77–90; https://doi.org/10.5004/dwt.2021.27585.
20. Sarasini, F.; Tirillò, J.; Maffei, G.; Zuorro, A.; Lavecchia, R.; Luzi, F.; Puglia, D.; Torre, L.; Maghchiche, A. Thermal and Mechanical Behavior of Thermoplastic Composites Reinforced with Fibers Enzymatically Extracted from Ampelodesmos Mauritanicus. *Polym. Eng. Sci.* **2019**, *59* (12), 2418–2428; https://doi.org/10.1002/pen.25093.
21. Zergane, H.; Abdi, S.; Xu, H.; Hemming, J.; Wang, X.; Willför, S.; Habibi, Y. Ampelodesmos Mauritanicus a New Sustainable Source for Nanocellulose Substrates. *Ind. Crop. Prod.* **2020**, *144*, 112044; https://doi.org/10.1016/j.indcrop.2019.112044.
22. Bourahli, M. E. H.; Osmani, H. Chemical and Mechanical Properties of Diss (*Ampelodesmos Mauritanicus*) Fibers. *J. Nat. Fibers.* **2013**, *10* (3), 219–232; https://doi.org/10.1080/15440478.2012.761115.
23. Nouri, M.; Griballah, I.; Tahlaiti, M.; Grondin, F.; Beaugrand, J. Plant Extraction and Physicochemical Characterizations of Untreated and Pretreated Diss Fibers (Ampelodesmos Mauritanicus). *J. Nat. Fibers* **2021**, *18* (8), 1083–1093; https://doi.org/10.1080/15440478.2019.1687062.
24. Sarasini, F.; Tirillò, J.; Maffei, G.; Zuorro, A.; Lavecchia, R.; Abdelhak, M. Enzyme-assisted Extraction of Fibres from Ampelodesmos Mauritanicus and Mechanical Characterization of Their Composites; *AIP Conf. Proc.*, **2018**, *1981* (1), 2002020024; https://doi.org/10.1063/1.5045882.
25. Rana, A. K.; Frollini, E.; Thakur, V. K. Cellulose Nanocrystals: Pretreatments, Preparation Strategies, and Surface Functionalization. *Int. J. Biol. Macromol.* **2021**, *182*, 1554–1581. https://doi.org/10.1016/j.ijbiomac.2021.05.119.
26. Benchikh, L.; Merzouki, A.; Grohens, Y.; Guessoum, M.; Pillin, I. Characterization of Cellulose Nanocrystals Extracted from El Diss and El Retma Local Plants and Their Dispersion in Poly(vinyl Alcohol-Co-Ethylene) Matrix in the Presence of Borax. *Polym. Polym. Compos.* **2021**, *29* (3), 218–230. https://doi.org/10.1177/0967391120910877.
27. Benchikh, L.; Merzouki, A.; Grohens, Y.; Pillin, I. Extruded Poly (Ethylene–co–vinyl Alcohol) Composite Films Reinforced with Cellulosic Fibers Isolated from Two Local Abundonates Plants. *J. Fundam. Appl. Sci.* **2020**, *12* (1), 49–72. https://doi.org/10.4314/jfas.v12i1.5.
28. Lin, N.; Huang, J.; Chang, P. R.; Feng, J.; Yu, J. Surface Acetylation of Cellulose Nanocrystal and its Reinforcing Function in Poly(lactic Acid). *Carbohydr. Polym.* **2011**, *83* (4), 1834–1842. https://doi.org/10.1016/j.carbpol.2010.10.047.
29. Trifol, J.; Plackett, D.; Sillard, C.; Hassager, O.; Daugaard, A. E.; Bras, J.; Szabo, P. A Comparison of Partially Acetylated Nanocellulose, Nanocrystalline Cellulose, and Nanoclay as Fillers for High-Performance Polylactid Nanocomposites. *J. Appl. Polym. Sci.* **2015**, *133* (14), 43257. https://doi.org/10.1002/app.43257.
30. Fortunati, E.; Puglia, D.; Mont, M.; Peponi, L.; Santulli, C.; Kenny, J. M.; Torre, L. Extraction of Cellulose Nanocrystals from Phormiumtenax Fibres. *J. Polym. Environ.* **2013**, *21* (2), 319–328. https://doi.org/10.1007/s10924-012-0543-1.
31. Neto, W. P. F.; Putaux, J. L.; Mariano, M.; Ogawa, Y.; Otaguro, H.; Pasquini, D.; Dufresne, A. Comprehensive Morphological and Structural Investigation of Cellulose I and II Nanocrystals Prepared by Sulphuric Acid Hydrolysis. *RSC, Adv.* **2016**, *6* (79), 76017–76027. https://doi.org/10.1039/C6RA16295A.
32. Lu, P.; Hsieh, Y. Preparation and Properties of Cellulose Nanocrystals: Rods, Spheres, and Network. *Carbohydr. Polym.* **2010**, *82* (2), 329–336. https://doi.org/10.1016/j.carbpol.2010.04.073.
33. Pineda-Pimentel, M. G.; Flores-Ramirez, N.; Sanchez, J. C. F.; Lvova, L. D. ; Garcia, S. R. V.; Garcia-Gonzalez, L. Theoretical Analysis and FTIR of Cellulose nanowhiskers/poly(ButylAcrylate). *Superficies y Vacío* **2016**, *29* (3), 83–86. https://doi.org/10.5281/zenodo.8108341.
34. Oh, S. Y.; Yoo, D. I.; Shin, Y.; Seo, G. FTIR Analysis of Cellulose Treated with Sodium Hydroxide and Carbon Dioxide. *Carbohydr. Res.* **2005**, *340* (3), 417–428. https://doi.org/10.1016/j.carres.2004.11.027.
35. Tang, Y.; Shen, X.; Yanjun, J. Z.; Guo, D.; Kong, F.; Zhang, N. Extraction of Cellulose Nano-Crystals from Old Corrugated Container Fiber Using Phosphoric Acid and Enzymatic Hydrolysis Followed by Sonication. *Carbohydr. Polym.* **2015**, *125*, 360–366. https://doi.org/10.1016/j.carbpol.2015.02.063.
36. Martinez-Sanz, M.; Olsson, R. T.; Lopez-Rubio, A.; Lagaron, M. J. Development of Electrospun EVOH Fibres Reinforced with Bacterial Cellulose Nanowhiskers. Part I: Characterization and Method Optimization. *Cellulose* **2010**, *18* (2), 335–347. https://doi.org/10.1007/s10570010-9471-1.
37. Eyley, S.; Thielemans, W. Surface Modification of Cellulose Nanocrystals. *Nanoscale* **2014**, *6* (14), 7764–7779. https://doi.org/10.1039/C4NR01756K.
38. Satyamurthy, P.; Jain, P.; Balasubramanya, R. H.; Vigneshwaran, N. Preparation and Characterization of Cellulose Nanowhiskers from Cotton Fibres by Controlled Microbial Hydrolysis. *Carbohydr. Polym.* **2010**, *83* (1), 122–129. https://doi.org/10.1016/j.carbpol.2010.07.029.
39. Khalil, H. P. S. A.; Davoudpour, Y.; Aprilia, N. A. S.; Mustapha, A.; Hossain, S.; Islam, N.; Dungani, R. Nanocellulose Based Polymer Nanocomposite: Isolation, Characterization Andapplications. In *Nanocellulose polymer nanocomposite*; Thakur, V. K., Ed.; Wiley Blackwell Scrivener Publishing: Hoboken, NJ, 2014; pp. 273–309.
40. Elanthikkal, S.; Gopala krishna panicker, U.; Varghese, S.; Guthrie, J. T. Cellulose Microfibres Produced from Banana Plant Wastes: Isolation and Characterization. *Carbohydr. Polym.* **2010**, *80* (3), 852–859. https://doi.org/10.1016/j.carbpol.2009.12.043.
41. Nath, R.; Pachuau, L. Wild Musa Spp. Pseudostem as a New Source of Cellulose Nanocrystals. *Cellulose Chem. Technol.* **2022**, *56* (7–8), 727–736. https://doi.org/10.35812/CelluloseChemTechnol.2022.56.64.
42. Roman, M.; Winter, W. T. Effect of Sulfate Groups from Sulfuric Acid Hydrolysis on the Thermal Degradation Behavior of Bacterial Cellulose. *Biomacromolecules* **2004**, *5*, 1671–1677. https://doi.org/10.1021/bm034519+.
43. Pandi, N.; Sonawane, S. H.; Kishore, K. A. Synthesis of Cellulose Nanocrystals (CNCs) from Cotton Using Ultrasound-Assisted Acid Hydrolysis. *Ultrason. Sonochem.* **2021**, *70*, 105353. https://doi.org/10.1016/j.ultsonch.2020.105353.
44. Ibrahim, I. K.; Hussin, S. M.; Al-Obaidi, Y. M. Extraction of Cellulose Nano Crystalline from Cotton by Ultrasonic and its Morphological and Structural Characterization. *Mater. Chem. Phys.* **2015**, *1* (2), 99–109. https://doi.org/10.12691/ijmcp-1-4-4.
45. Peng, B. L.; Dhar, N.; Liu, H. L.; Tam, K. C. Chemistry and Applications of Nanocrystalline Cellulose and its Derivatives: A Nanotechnology Perspective. *Can. J. Chem. Eng.* **2011**, *89* (5), 1191–1206. https://doi.org/10.1002/cjce.20554.

46. Chirayil, C. J.; Mathew, L.; Thomas, S. Review of Recent Research in Nano Cellulose Preparation from Different Lignocellulosic Fibers. *Rev. Adv. Mater. Sci.* **2014**, *37*, 20–28. https://doi.org/10.1515/rams-2014-0002.
47. Benchikh, L.; Aitferhat, Y.; Kebaili, M.; Chorfi, H.; Abacha, I.; Guessoum, M.; Merzouki, A.; Benia, H. M.; Grohens, Y. Acetylation of Cellulose Nanocrystals Extracted from Cotton for Drilling Fluid Application: Structural and Thermal Characterization. *Int. J. Nanosci.* **2023**, *22* (5), 2350036. https://doi.org/10.1142/S0219581X23500369.
48. Guoa, J.; Duc, W.; Wang, S.; Yin, Y.; Gao, Y. Cellulose Nanocrystals: a Layered Host Candidate for Fabricating Intercalated Nanocomposites. *Carbohydr. Polym.* **2017**, *157*, 79–85. https://doi.org/10.1016/j.carbpol.2016.09.065.
49. Benchikh, L.; Aouissi, T.; Aitferhat, Y.; Chorfi, H.; Abacha, I.; Kebaili, M.; Guessoum, M.; Merzouki, A.; Grohens, Y.; Carraro, M.; Djellali, S. Effect of Different Compatibilization Routeson the Mechanical, Thermal and Rheological Propertiesof Polypropylene/cellulose Nanocrystals Nanocomposites. *Polym. Bull.* **2024**, *81*, 11007–11026; https://doi.org/10.1007/s00289-024-05225-w.
50. Razalli, R. L.; Abdi, M. M.; Tahir, P. M.; Moradbak, A.; Sulaiman, Y.; Heng, L. Y. Polyaniline-modified Nanocellulose Prepared from Semantan Bamboo by Chemical Polymerization: Preparation and Characterization. *RSC Adv.* **2017**, *7* (41), 25191–25198. https://doi.org/10.1039/C7RA03379F.
51. Varma, R.; Vasudevan, S. Extraction and Characterisation of Cellulose from Red Seaweeds of Hypnea Musciformis and Sarconema Filliforme. *Cellulose Chem. Technol.* **2022**, *56* (9–10), 949–956. https://doi.org/10.35812/CelluloseChemTechnol.2022.56.03.
52. Law, Y. N.; Ting, J. W.; Ching, Y. N.; Chiang, K. M. A. A Review on Cellulose Nanocrystals Production and Characterization Methods from Elaeis Guineensis Empty Fruit Bunches. *Arab. J. Chem.* **2021**, *14* (9), 103339–103364. https://doi.org/10.1016/j.arabjc.2021.
53. Beyene, D.; Chae, M.; Dai, J.; Danumah, C. H.; Tosto, F.; Demesa, A. G.; Bressler, D. C. Characterization of Cellulase-Treated Fibers and Resulting Cellulose Nanocrystals Generated through Acid Hydrolysis. *Mater* **2018**, *11* (8), 1272–1288. https://doi.org/10.3390/ma11081272.
54. Ferreira, F. V.; Pinheiro, I. F.; Gouveia, R. F.; Thim, G. P.; Lona, L. M. F. Functionalized Cellulose Nanocrystals as Reinforcement in Biodegradable Polymer Nanocomposites. *Polym. Compos.* **2018**, *39* (1), E9–E29. https://doi.org/10.1002/pc.24583.